Molecular Crystals and Liquid Crystals

Publication details, including instructions for authors and subscription information:
http://www.tandfonline.com/loi/gmcl20

Organic Semiconductors with Helical Structure Based on Oligothiophene derivatives Exhibiting Chiral Nematic Phase

Dr. Masahiro Funahashi [a] & Dr. Nobuyuki Tamaoki [a]

[a] Molecular Smart System Group, Nanotechnology Research Institute, National Institute of Advanced Industrial Science and Technology Tsukuba, Ibaraki, Japan

Version of record first published: 22 Sep 2010

To cite this article: Dr. Masahiro Funahashi & Dr. Nobuyuki Tamaoki (2007): Organic Semiconductors with Helical Structure Based on Oligothiophene derivatives Exhibiting Chiral Nematic Phase, Molecular Crystals and Liquid Crystals, 475:1, 123-135

To link to this article: http://dx.doi.org/10.1080/15421400701735723

Mol. Cryst. Liq. Cryst., Vol. 475, pp. 123–135, 2007

ISSN: 1542-1406 print/1563-5287 online
DOI: 10.1080/15421400701735723

Taylor & Francis
Taylor & Francis Group

Organic Semiconductors with Helical Structure Based on Oligothiophene derivatives Exhibiting Chiral Nematic Phase

Dr. Masahiro Funahashi
Dr. Nobuyuki Tamaoki
Molecular Smart System Group, Nanotechnology Research Institute, National Institute of Advanced Industrial Science and Technology
Tsukuba, Ibaraki, Japan

*We have synthesized 2-[5-(4-[(S)-2-methylbutoxy]phenyl)-3-methyl]-2‴-propyl-2:5′-2′:5″-2″:5‴-quaterthiophene (**10**), a liquid crystalline semiconductor that exhibits a chiral nematic phase, and used the time-of-flight technique to determine its carrier mobility behavior. In the chiral nematic phase, the positive carrier mobility was 2×10^{-4} cm^2/Vs at 120°C and the negative carrier mobility was 1×10^{-4} cm^2/Vs, both of which we attribute to electronic processes. For the negative carrier, in addition to the fast electronic process, we also observed a slow carrier transport, having mobility on the order of 10^{-5} cm^2/Vs, which we attribute to ionic conduction. Chiral dimers containing binaphthyl group exhibited stable glassy cholesteric phase and cholesteric thin films with selective reflection band in visible light area could be fabricated. They emitted circularly polarized light with dichroic parameter of 1.3 when UV light was illuminated.*

Keywords: carrier mobility; cholesteric; electronic conduction; organic semiconductors; selective reflection; time-of-flight technique

INRTODUCTION

Cholesteric liquid crystals (CLCs) are promising optical materials for reflective displays [1] and imaging devices [2] because the periodicities of their helical structures are on the order of the wavelengths in visible light. Circularly polarized light photoluminescence [3] and

We thank the Association for the Progress of New Chemistry, Sumitomo Foundation, and Grant in Aid for Scientific Research (No. 16750185) for financial support.

Address correspondence to Masahiro Funahashi, Molecular Smart System Group, Nanotechnology Research Institute, National Institute of Advanced Industrial Science and Technology, Tsukuba Central 5-2, Higashi 1-1-1, Tsukuba, Ibaraki 305-8563, Japan.
E-mail: Masahiro-funahashi@aist.go.jp

laser emission from cholesteric liquid crystals have been investigated recently [4–7], but only optical pumping was possible in these studies in which fluorescent dyes were doped in the cholesteric matrixes. The realization of electrical pumping systems, which are more practical, requires the construction of semiconductive cholesteric systems.

Electronic charge carrier transport has been confirmed in smectic systems [8–12] and discotic columnar phases [13–16] in which intermolecular packing structures promote intermolecular electronic charge transfer. In contrast, only ionic conduction caused by contamination of ionic impurity has been observed in nematic or cholesteric phases [17–23], which exhibit more liquid-like fluidity than do smectic and discotic mesophases. Electronic conduction has also been observed in the glassy nematic phases of some low- and high-molecular-weight materials [24,25]. In particular, the glassy chiral nematic phase of a fluorene derivative exhibited good hole transporting properties, with mobility on the order of $10^{-4}\,cm^2/Vs$, in addition to luminescence of circularly polarized light [25].

Ionic processes should be dominant in achiral and chiral nematic phases that possess lower viscosities and have intermolecular transfer integrals smaller than those of smectic phases. Increasing the transfer integral should be an effective approach to realizing electronic conduction in nematic and chiral nematic phases. Recently, electronic conduction was confirmed in fluidic chiral nematic [26] and achiral nematic phases [27] of oligothiophene derivatives with extended π-conjugated system. However the detailed mechanism of electronic charge carrier transport in these phases has been unclear. In addition, for practical application of the liquid crystalline semiconductors with helical structure to opt-electronics devices, fixation of helical order at room temperature is indispensable and the helical pitch should be tuned by temperature or other method.

In this article, we report electronic charge carrier transport characteristics in the fluidic chiral nematic phase of an oligothiophene derivative as well as synthesis and circularly polarized light emission of dimeric oligothiophene derivatives containing binaphthyl group as a chiral moiety.

MATERIALS

In this study, we investigated carrier transport characteristics of [5-(4-[(*S*)-2-methylbutoxy]phenyl)-3-methyl]-2‴-propyl-2:5′-2′:5″-2″:5‴-quaterthiophene (**10**) as shown in Scheme 1. We adopted the 5-phenyl-2:5′-2′:5″-2″:5‴-quarter-thiophene skeleton as an aromatic core having

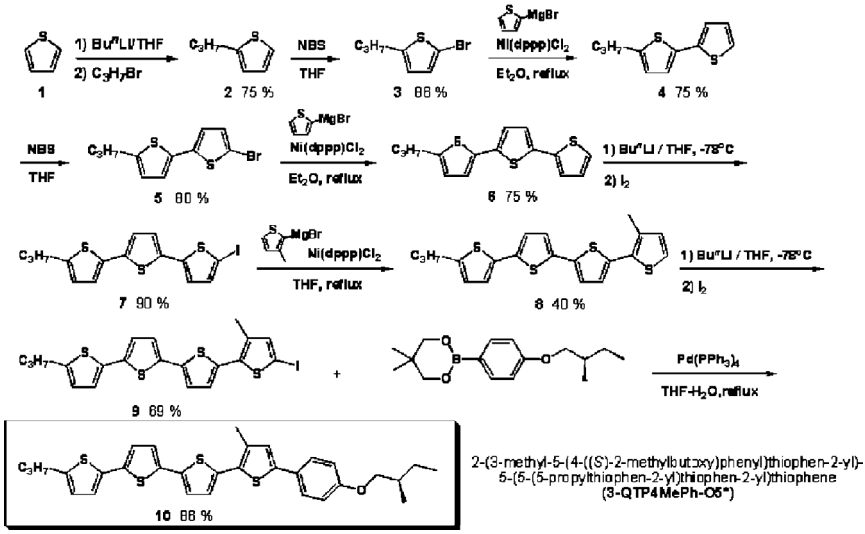

SCHEME 1 Synthetic route toward 2-[5-(4-[(*S*)-2-methylbutoxy]phenyl)-3-methyl]-2‴-propyl-2:5′-2′:5″-2″:5‴-quaterthiophene.

a large π-conjugated system; for alkyl chains that induce mesophases, we used short propyl and (*S*)-2-methylbutyl groups.

In the DSC measurements of **10**, small exo- and endo-thermal peaks ($\Delta H = 1.2\,J/g$), which are characteristic of isotropic-nematic and isotropic-chiral nematic transitions, appeared at 182°C during the cooling and heating cycles. At 83°C, a large exothermal peak ($\Delta H = 54\,J/g$), which corresponds to crystallization, appeared during the cooling process. In X ray diffraction, only a broad hallo associated with liquid-like order was observed around $2\theta = 20$ degrees without sharp peaks in low angle region in the mesophase, indicating the mesophase is nematic or chiral nematic phase. No cybotactic peaks were not observed in low angle region, indicating no microscopic smectic-like order formation in the phase. For observation of optical textures under a polarized light microscope, we prepared liquid crystal cells (thicknesses: 9 μm) on two ITO-coated glass plates. In the absence of an electric field we observed a Granjan texture, which is characteristic of a chiral nematic phase, in the mesophase of **10**, indicating a planar alignment of the liquid crystal molecules. After applying an electric field (applied voltage $>10\,V$) to the 9-μm-thick sample, we observed a fingerprint texture, indicating that the helical axis was parallel to the electrode surface. The molecules of the compound **10** have a

tendency to align parallel to the electric field because the molecule has induced dipole moment along the molecular axis although its permanent dipole is perpendicular to the axis. From the periodicity of the observed fingerprint texture, the helical pitch was ca. 7 μm, i.e., it was comparable to the thickness of the sample (9 μm). The helical twisting power of **10** should not be so large as to induce a helical structure having a short periodicity. Under strong electric field, we observed the change of the direction of the helical axis from perpendicular to parallel to the surface when electric field was applied. We performed the electrical measurements in such an alignment that the helical axis was parallel to the electrode surface.

CHARACTERIZATION OF CARRIER TRANSPORT IN THE CHIRAL NAMTIC PHASE

We determined the carrier mobility through the use of a conventional time-of-flight technique [31]; the apparatus consisted of a pulse laser (THG of a Nd:YAG laser; wavelength, 355 nm; pulse duration, 1 ns) for excitation, the sample on a hot stage, a serial resistor, and a digital oscilloscope. All measurements were carried out under atmospheric condition. The electric field was applied to the liquid crystal cell consisting of two ITO-coated glass plates. The pulse laser illuminated one side of the cell. When the absorption coefficient of a sample is sufficiently large, the excitation pulse is absorbed and a sheet of photocarriers is generated near the illuminated electrode. In this study, the neat film of **10** exhibits strong absorption band around 400 and 250 nm in the chiral nematic phase at 120°C; the depth of penetration of the excitation light at 356 nm was estimated to be less than 0.5 μm, i.e., it was much smaller than the sample thickness. Under the influence of the electric field, the photogenerated carriers drifted across the bulk of the sample, inducing a displacement current through the serial resistor. When the charge carriers arrived at the counter electrode, the induced displacement current decreased to zero. Therefore, a kink point in a transient photocurrent curve corresponds to the transit time t_T. Using equation (1), the carrier mobility (μ) can be calculated from the values of t_T, the sample thickness d, and the applied voltage V:

$$\mu = \frac{d^2}{Vt_T} \tag{1}$$

Illuminating the electrode under a positive or negative bias allows the positive or negative carrier mobility to be determined, respectively.

RESULT AND DISCUSSION

For the quaterthiophene derivative **10**, we measured the transient photocurrents for the positive and negative carriers—in both the isotropic and chiral nematic phases—at temperatures from 220 to 90°C.

For positive carriers, we obtained non-dispersive transient photocurrent curves for the isotropic and chiral nematic phases, as indicated in Figure 1. The kink point in each transient photocurrent curve shifted according to the applied electric field, indicating that the transient photocurrents originated through carrier transport in the bulk of the sample. At 120 °C and under an electric field of 5×10^4 V/cm, the positive carrier mobility was 2×10^{-4} cm^2/Vs. This value is approximately one order of magnitude higher than the ionic mobility in conventional nematic liquid crystals, and it is comparable to that found in the glassy nematic phases of fluorene derivatives.

For negative carriers, we also obtained transient photocurrent curves with kink points over the entire temperature range, but the results presented in Figure 2 are somewhat more complicated. In the isotropic phase, we observed non-dispersive transient photocurrents in the longer time range that had mobilities of 10^{-5} cm^2/Vs. In the chiral nematic phase, we obtained non-dispersive curves in almost the same time range at temperatures above 170 °C, but the transient curves became ambiguous upon decreasing the temperature below

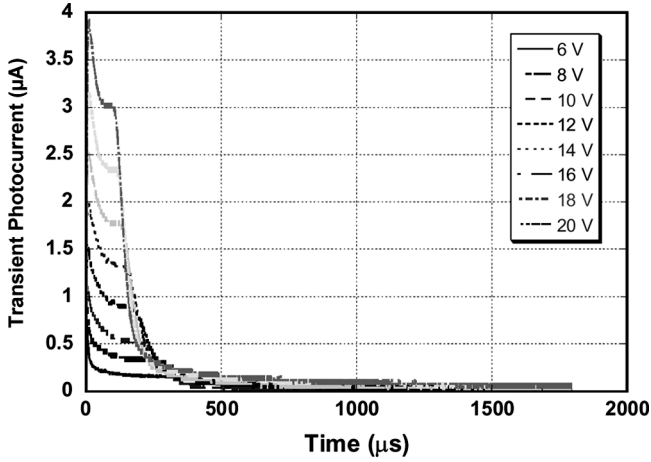

FIGURE 1 Transient photocurrent curves for positive carriers at 120 °C (chiral nematic phase). Sample thickness, 4 μm; wavelength of excitation, 355 nm.

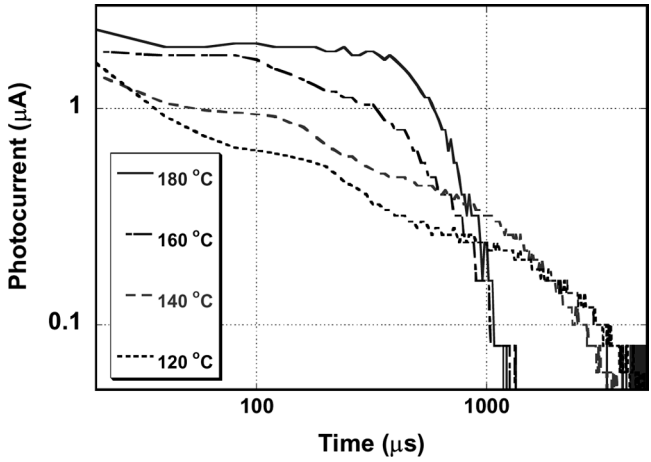

FIGURE 2 Transient photocurrent curves for negative carriers at 50 V at various temperatures. Sample thickness, 9 μm; wavelength of excitation, 355 nm.

170 °C, and another transit, at a shorter time range, in addition to that at the longer time range, appeared at temperatures below 150 °C. The both kink points appeared at a shorter and longer time range shift to shorter time when electric field increased and these kink points should be therefore attributed to carrier transport. The negative carrier mobility in the shorter time range was $2 \times 10^{-4}\,cm^2/Vs$ and that in longer time range was $4 \times 10^{-5}\,cm^2/Vs$. The former value is comparable to the positive carrier mobility of this material at the same temperature and electric field. The latter value is approximately one order of magnitude lower than the positive carrier mobility of this compound, but it is on the same order of magnitude of the ionic carrier mobilities of conventional nematic liquid crystals.

Figure 3 displays a plot of the carrier mobility as a function of the electric field and temperature. The positive carrier mobility increased and eventually became saturated upon increasing the temperature, but then a discontinuous decrease in the positive carrier mobility occurred at the temperature of the transition from the chiral nematic to the isotropic phase.

In contrast to the positive carrier, the negative carrier mobility at the longer time range increased monotonically upon increasing the temperature. This change was continuous at the phase transition temperature, indicating that the positive and negative carriers undergo different transport mechanisms. The negative carrier mobility at the

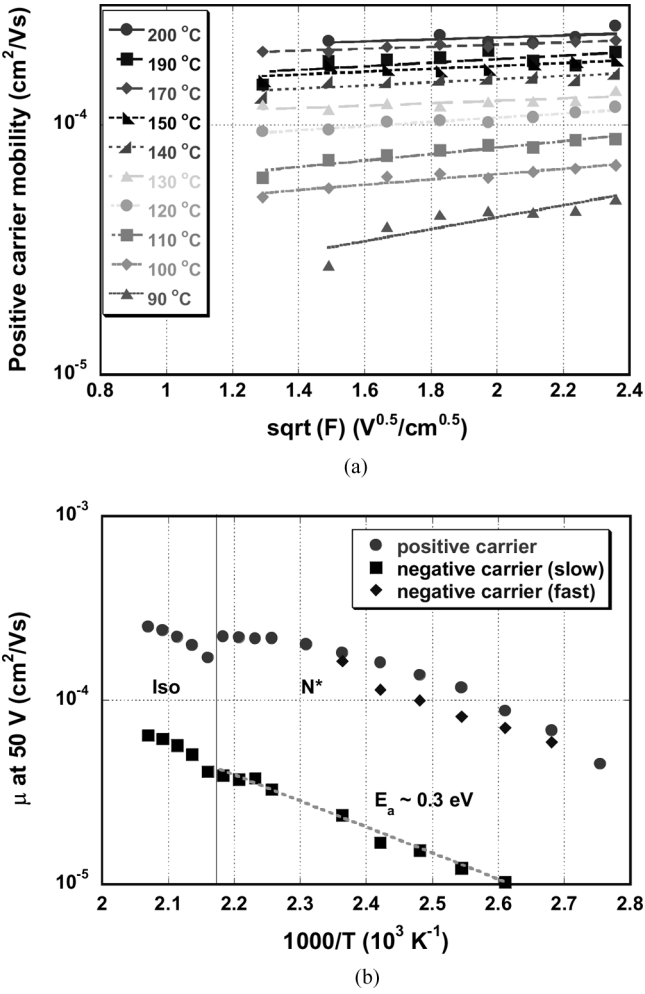

FIGURE 3 Positive carrier mobilities plotted as functions of the (a) electric field and (b) temperature.

shorter time range exhibited a positive dependence on the temperature, indicating a thermal activation process.

The viscosity of compound **10** at 130 °C, which we measured using a capillary viscometer, was 0.6 poise, almost the same as that in the nematic phase of 5CB at room temperature; in that case, ionized 5CB molecules or smaller metal ions were assumed to be the charge carriers [21]. The carrier mobility in the nematic phase of 5CB, as

determined through TOF and AC conductivity measurements, is on the order of 10^{-6} to $10^{-5}\,cm^2/Vs$ [20,21]. Therefore, the ionic mobility in the chiral nematic phase of **10** should be on the order of 10^{-5} or smaller, assuming that the ionic charge carriers are the ionized liquid crystal molecules. The measured positive carrier mobility, and the negative one at shorter time range, was $1.5 \times 10^{-4}\,cm^2/Vs$, which is one order of magnitude larger than the predicted value; the negative carrier mobility at the longer time scale was on the same order as the predicted value. This result implies that the positive and negative carrier transport at the shorter time range was electronic in nature and that the negative carrier transport at the longer time range was ionic in nature if the size of the ionic species was on the same order.

The positive carrier mobility decreased during the transition from the chiral nematic phase to the isotropic phase upon increasing the temperature. In this study, the helical axis of the chiral nematic phase was aligned parallel to the electrode surface under the applied electric field, and the helical pitch was comparable in size to the sample thickness. Therefore, we regarded the molecular alignment as being in a nematic-like state consisting of areas in which the molecular axes were vertical and parallel to the electrode surface. For ionic transport in the nematic phase, the carrier mobility along and perpendicular to the director was measured using the time-of-flight method and through AC conductivity measurements in samples aligned with the magnetic field. The carrier mobility along the director increased almost continuously, or decreased slightly, at the point of transition from the nematic to the isotropic phase upon increasing the temperature, whereas the carrier mobility perpendicular to the director increased discontinuously at that point upon increasing the temperature [17–23]. The mobility along the director was larger than that perpendicular to the director, but the anisotropy was small (at 1.5–2, at best) [17,21]. The discontinuous decrease in the measured positive carrier mobility at the transition point should be attributed to an increase in the disorder and a decrease in the transfer integral based on electronic, rather than ionic, conduction. The change at the phase transition temperature was, however, only 1.7, which is much smaller than the changes observed at the temperatures of transition between the smectic and isotropic phases of 2-phenylnaphthalene and terthiophene derivatives [9,10]. This phenomenon arises because these phases are more liquid-like than are the smectic phases.

The negative carrier mobility at the longer time range increased continuously at the phase transition temperature upon increasing the temperature; this behavior is typical for ionic mobility along the director in the nematic phase [17,21,22]. Therefore, ionic conduction

should be valid for negative carrier transport at the longer time range in the chiral nematic and isotropic phases.

In addition, the temperature dependence of the positive carrier mobility within the chiral nematic phase of **10** also indicates that electronic process should be dominant for positive carrier transport in this phase. In the nematic and chiral nematic phases, the viscosity decreases monotonically upon increasing the temperature and, therefore, the ionic carrier mobility should increase monotonically [17,20,21]. As measured using a capillary viscometer, we found that the viscosity increased monotonically upon increasing the temperature within the chiral nematic phase of **10**. From the Arrhenius plot of the logarithm of inverted viscosity against 1/T, we estimated the activation energy to be 0.3 eV. For negative carrier transport, the Arrhenius plot confirmed that linearity existed between the logarithm of the negative carrier mobility at longer time range and 1/T; the activation energy of 0.3 eV is identical to that of the viscosity. This result supports the notion that negative carrier transport at the longer time range is based on an ionic process. The ionic carriers in this process are possibly impurities or liquid crystal molecules that were ionized upon illumination with the laser. In contrast, the positive carrier mobility exhibits saturation upon increasing the temperature, possibly because of competition between thermally activated intermolecular electron transfer and structural disorder caused by molecular movement in the electronic carrier transport process, but not in the ionic case. Such saturation in hole mobility with respect to temperature has been observed for discotic columnar and smectic phases [12,14].

The results of this study indicate that extending the π-conjugated of a system is an effective means of realizing electronic conduction in chiral nematic phases. In the nematic and chiral nematic phases of conventional liquid crystals, however, the π-conjugated systems are not sufficiently large and, therefore, they exhibit small intermolecular transfer integrals and low viscosities. Consequently, only ionic carrier transport has been observed previously in nematic and cholesteric phases.

SYNTHESIS AND PHASE TRANSITION BEHAVIOR OF CHIRAL DIMERS 14 AND 15

Compound **10** crystallizes at room temperature and cannot retain the chiral nematic phase. Dimeric compounds which exhibit glassy cholesteric phase below room temperature have been reported by N. Tamaoki [2]. In this study, chiral dimeric oligothiophene derivatives

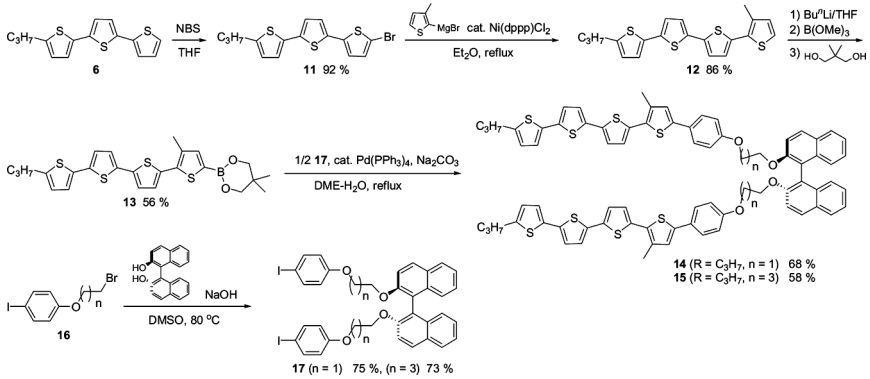

SCHEME 2 Synthetic route toward chiral dimer **14** and **15**.

containing binaphthyl group as a chiral moiety **14** and **15** were designed and syntheized. They were synthesized by Pd(0)-catalyzed Suzuki coupling reaction between propylquaterthienyl boric acid 2,2-propanediyl ester **13** and binaphthyl derivatives **17** as shown in Scheme 2.

PHASE TRANSITION BEHAVIOR OF CHIRAL DIMMERS

Phase transition behaviors of these chiral dimmers were characterized by optical texture observation under polarized light microscope and differential scanning caloriemetry (DSC). In DSC measurement, dimer **14** and **15** exhibited a single transition peak corresponding to the isotropic to cholesteric phase at 163 °C and 155 °C respectively. Below the transition peak, they exhibited glass transition at 72 °C and 57 °C respectively. From X ray diffraction, only broad hallo around $2\theta = 20$ degree was observed in the cholesteric phase of these compounds, indicating they have no smectic order. Under polarized light microscope, Granjan texture was observed, which is characteristic for cholesteric phase.

REFLECTION SPECTRA OF THE DIMERIC COMPOUNDS

Dimer **14** and **15** exhibited selective reflection band in visible light wavelength area. And the selective reflection band of these compounds can be tuned from near infrared to ultraviolet area by temperature and mixing with monomeric compound. Figure 4 shows reflection spectrum of the mixture of dimer **15** and monomeric compound **10** at various temperature. It should be noted that the wide reflection band

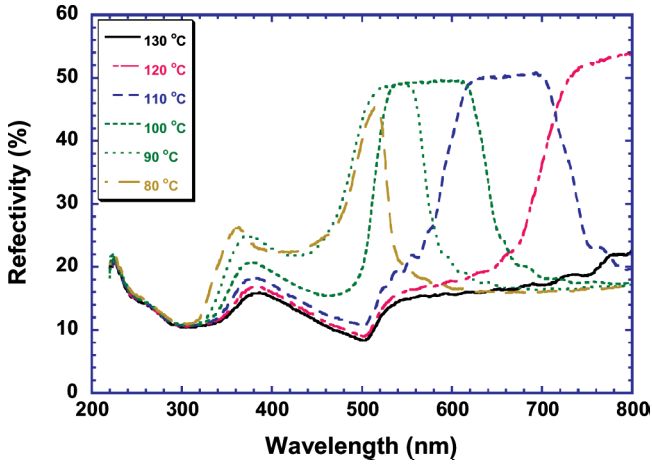

FIGURE 4 Selective reflection spectra of the 1:1 mixture of **10** and **15** at various temperature.

width exceeding over 100 nm and broad tunability from near infrared to ultraviolet area. This prominent properties should be attributed to large anisotropy in refractive index due to long extended π-conjugated system. Therefore we can fabricate cholesteric thin films with various reflection colors.

CIRCULARLY POLARIZED PHOTOLUMINESCENCE FROM THE CHOLESTERIC FILMS

Circularly polarized light photoluminescence from cholesteric films was reported by Chen *et al*. [33]. and M. O'Neill who reported circularly polarized light photoluminescence from glassy cholesteric semiconductor with wide wavelength range [3].

The mixture of dimer **15** and monomeric compound **10** form well aligned cholesteric thin film could be fabricated on substrates on which rubbed polyimide film was coated. Circularly polarized photoluminescence was observed through a filter consisting of $\lambda/2$ and $\lambda/4$ plates, illuminating UV light (wavelength = 356 nm) from the back side of the film sample. Figure 5 shows circularly polarized light spectra from the 1:1 mixture. These compounds have photoluminescence band between 500 and 700 nm and exhibit orange color. Within the reflection band, circularly polarized luminescence with different helicity from the cholesteric film was suppressed, while circularly polarized luminescence with same helicity was emitted with no change.

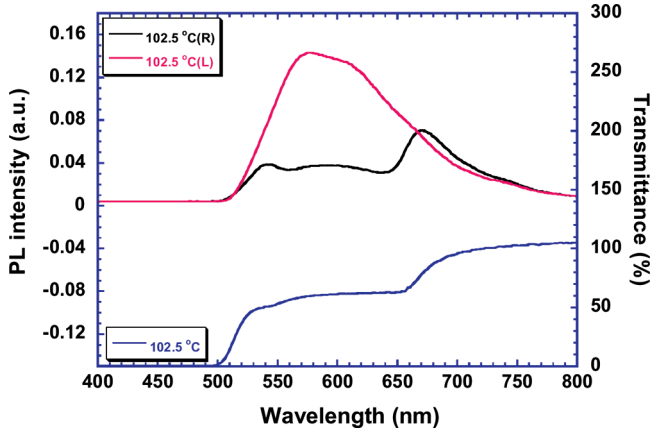

FIGURE 5 Circularly polarized photoluminescence of the 1:1 mixture of **10** and **15** at 102.5°C.

The circularly polarization parameter reached up to 1.3. At the band edge, distortion in the spectrum of with different helicity from the cholesteric film was observed. This distortion is associated with laser emission. These cholesteric film can transport hole and they should be applied electrically-pumped opt-electronics devices.

In conclusion, we have synthesized a liquid crystalline semiconductor, 2-[5-(4-[(*S*)-2-methylbutoxy]phenyl)-3-methyl]-2‴-propyl-2:5′-2′:5″-2″:5‴-quaterthiophene (**10**), which exhibits a chiral nematic phase. We used the time-of-flight technique to determine its carrier mobility. In the chiral nematic phase, the positive carrier mobility was $2 \times 10^{-4}\,cm^2/Vs$ at 120 °C and the negative carrier mobility was $1 \times 10^{-4}\,cm^2/Vs$; they are both attributed to electronic processes. For the negative carrier, in addition to the fast electronic process, we also observed a slow carrier transport having mobility on the order of $10^{-5}\,cm^2/Vs$, which we attribute to ionic conduction.

Chiral dimers **14** and **15** containing binaphthyl group exhibited glassy cholesteric phase around room temperature and cholesteric thin films with selective reflection band in visible light area could be fabricated. They emitted circularly polarized light when UV light was illuminated. The dichroic parameter reached up to 1.3.

REFERENCES

[1] Yang, D. K., Chien, L. C., & Doane, J. W. (1991). *IDRC, Proc*, 49–55.
[2] Tamaoki, N., Parfenov, A. V., Masaki, A., & Matsuda., H. (1997). *Adv. Mater.*, *9*, 1102–1104.

[3] Woon, K. L., O'Neill, M., Richards, G. J., Aldred, M. P., Kelly, S. M., & Fox, A. M. (2003). *Adv. Mater.*, *15*, 1555–1558.
[4] Finkelmann, H., Kim, S. T., Muñoz, A., Palffy-Muhoray, P., & Taheri, B. (2001). *Adv. Mater.*, *13*, 1069–1072.
[5] Furumi, S., Yokoyama, S., Otomo, A., & Mashiko, S. (2004). *Appl. Phys. Lett.*, *84*, 2491–2493.
[6] Araoka, F., Shin, K., Takanishi, Y., Ishikawa, K., & Takezoe, H. (2003). *J. Appl. Phys.*, *94*, 279–281.
[7] Ozaki, M., Kasano, M., Ganzke, D., Haase, W., & Yoshino, K. (2002). *Adv. Mater.*, *14*, 306–309.
[8] Funahashi, M. & Hanna, J. (1997). *Phys. Rev. Lett.*, *78*, 2184–2187.
[9] Funahashi, M. & Hanna, J. (1997). *Appl. Phys. Lett.*, *71*, 602–604.
[10] Funahashi, M. & Hanna, J. (2000). *Appl. Phys. Lett.*, *76*, 2574–2576.
[11] Funahashi, M. & Hanna, J. (2005). *Adv. Mater.*, *17*, 594–598.
[12] Funahashi, M. and Hanna, J. (2001). *Mol. Cryst. Liq. Cryst.*, *368*, 4071–4078.
[13] Adam, D., Closs, F., Frey, T., Funhoff, D., Haarer, D., Ringsdorf, H., Schuhmacher, P., & Siemensmeyer, K. (1993). *Phys. Rev. Lett.*, *70*, 457–460.
[14] Adam, D., Schuhmacher, P., Simmerer, J., Häußling, L. H., Paulus, W., Siemensmeyer, K., Etzbach, K. H., Ringsdorf, H., & Haarer, D. (1995). *Adv. Mater.*, *7*, 276–280.
[15] van de Craats, A. M., Warman, J. M., Müllen, K., Geerts, Y., & Brand, J. D. (1998). *Adv. Mater.*, *10*, 36–38.
[16] Pecchia, A., Lozman, O. R., Movaghar, B., Boden, N., & Bushby, R. (2002). *Phys. Rev. B*, *65*, 104204.
[17] Yoshino, K., Tanaka, N., & Inuishi, Y. (1976). *Jpn. J. Appl. Phys.*, *15*, 735–736.
[18] Shimizu, Y., Shigeta, K., & Kusabayashi, S. (1986). *Mol. Cryst. Liq. Cryst.*, *140*, 105–117.
[19] Heilmeyer, G. H. & Heyman, P. M. (1969). *Phys. Rev. Lett.*, *18*, 583–586.
[20] Murakami, S., Naito, H., Okuda, M., & Sugiyama, A. (1995). *J. Appl. Phys.*, *78*, 4533–7537 .
[21] Sawada, A., Manabe, A., & Naemura, S. (2001). *Jpn. J. Appl. Phys.*, *40*, 220–224.
[22] Yoshino, K., Yamashiro, K., & Inuishi, Y. (1974). *Jpn. J. Appl. Phys.*, *13*, 1471–1472.
[23] Sawada, A. & Naemura, S. (2002). *Jpn. J. Appl. Phys.*, *41*, L195-L197 .
[24] Ikeda, T., Mochizuki, H., Hayashi, Y. Sisido, M., & Sasakawa, T. (1991). *J. Appl. Phys.*, *70*, 3696–3702.
[25] Farrar, S. R., Contoret, A. E. A., O'Neill, M., Nicholls, J. E., Richards, G. J., & Kelly, S. M. (2002). *Phys. Rev. B*, *66*, 125107.
[26] Woon, K. L., Aldred, M. P., Vlachos, P., Mehl, G. H., Stimer, T., Kelly, S. M., & O'Neill, M. (2006). *Chem Mater.*, *18*, 2311.
[27] Funahashi, M. & Tamaoki, N. (2006). *Chem. Phys. Chem.*, *7*, 1193–1197.
[28] Garnier, F., Hajlaoui, R., Kassmi, A. E., Horowitz, G., Laiyre, L., Porzio, W., Armanini, A., & Provasoli, F. (1998). *Chem. Mater.*, *10*, 3334–3339.
[29] Ponomarenko, S. & Kirchmeyer, S. (2003). *J. Mater. Chem.*, *13*, 197–202.
[30] Geng, Y., Fechtenköttner, A., & Müllen, K. (2000). *J. Mater. Chem.*, *11*, 1634–1641.
[31] Kepler, R. G. (1960). *Phys. Rev.*, *119*, 1226–1229.
[32] Chandrasekhar, S. (1992). *Liquid Crystals*, Cambridge: Cambridge University Press.
[33] Chen, S. H., Katsis, D., Schmid, A. W., Mastrangelo, J. C., Tsutsui, T., & Blanter, T. N. (1999). *Nature*, *397*, 506.